

# Prediction of the Hydration Properties of Diamondoids from Free Energy and Potential of Mean Force Calculations

Cleiton Maciel,<sup>†</sup> Thaciana Malaspina,<sup>‡</sup> and Eudes E. Fileti<sup>\*,§</sup>

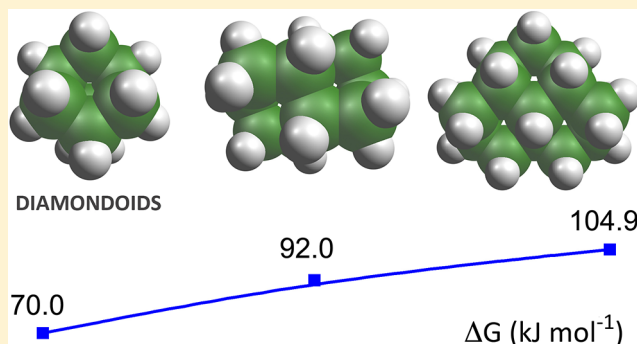
<sup>†</sup>Centro de Ciências Naturais e Humanas, Universidade Federal do ABC, 09210-270 Santo André, SP, Brazil

<sup>‡</sup>Instituto do Mar, Universidade Federal de São Paulo, 11030-400, Santos, SP, Brazil

<sup>§</sup>Instituto de Ciência e Tecnologia, Universidade Federal de São Paulo, 12231-280, São José dos Campos, SP, Brazil

## S Supporting Information

**ABSTRACT:** Molecular dynamics simulations were used to predict the thermodynamical properties of the hydration process of the adamantane, diamantane, and trimantane, the first three members of the series of diamondoids. Free-energy results suggest that the water solubility of these molecules is low. The hydration free energy increases with size of the diamondoid. As for the alkane hydrocarbons, hydration free energy correlates linearly with the surface accessible solvent area; however, here it has been shown that small diamondoids present hydration free energy significantly lower than the *n*-alkanes of similar molecular weights. The decomposition of the hydration free energy in enthalpic and entropic terms revealed that the hydration process of the small diamondoids is entropic driven. The potential of mean-force calculations indicates that the aggregation of these species in the aqueous medium should occur spontaneously and that the contribution of the solvent is greater the larger the diamondoid.



## INTRODUCTION

Diamondoids can be considered to be pieces of diamond saturated with hydrogen.<sup>1–3</sup> These species have attracted attention because of their physical properties that make them potential materials for applications in petroleum industry,<sup>4</sup> nanotechnology,<sup>5</sup> and biomedical sciences.<sup>3</sup> Recently, the solubility of small diamondoids has been investigated because of its important role in the design of crystallization-based separation processes to recover the diamondoids from petroleum.<sup>6,7</sup> For instance, a practical problem with high-melting solid deposits during fractional distillation of oil has motivated an extensive investigation of high-pressure phase equilibrium in binary diamondoid–gas mixtures as well as determinations of solubility of diamondoids in supercritical fluids and in liquid hydrocarbons.<sup>6</sup> In parallel, solubility data of diamantane, trimantane, tetramantane, and their derivatives in various organic solvents, as measured by a solid disappearance method, revealed some of the characteristics of this class of compounds, which can be exploited for process design.<sup>7</sup> Additionally, diamondoids are being considered for biomedical applications,<sup>3</sup> and to this end the description of molecular interactions of these systems in condensed medium, particularly in water, is of crucial importance.

Despite the relevance of these molecular species and the attention they have received in recent years, few studies on its thermodynamic solvation are available. There are only few experimental studies on the solubility of diamondoids,<sup>6,8</sup> particularly under ambient conditions. From the computational

point of view, with the exception of a study of Scheraga and coworkers on the hydrophobic hydration of adamantane,<sup>9</sup> there is no other work devoted to quantify the properties of solvation of these species.

Molecular dynamics (MD) simulation is a powerful tool to describe or predict molecular and thermodynamic properties in solution. MD simulations can be safely used to describe the energetics and dynamics of hydration of diamondoids, allowing the characterization of the microscopic structure of solvation around the solute. Additionally, MD can be applied to investigate thermodynamic aspects related to the hydrophobic hydration. In this work, we perform computer simulations for the three simplest diamondoids (namely, adamantane, diamantane, and trimantane) in water to predict their hydration and association properties. To get insight into the solubility of these systems, we carried out free-energy calculations and analysis in terms of its enthalpic and entropic components. Aiming at the characterization of diamondoid aggregation in water, we determine the potential of mean force (PMF) for each pair of diamondoid as a function of the distance between the center of mass. In all cases a careful analysis of the diamondoid size dependence was performed.

**Received:** August 9, 2012

**Revised:** October 17, 2012

**Published:** October 18, 2012

## SIMULATION DETAILS

MD simulations of the aqueous solutions of C<sub>10</sub>H<sub>16</sub> (adamantane, ADA), C<sub>14</sub>H<sub>20</sub> (diamantane, DIA), and C<sub>18</sub>H<sub>24</sub> (trimantane, TRI) were performed in the NPT ensemble with  $T = 298$  K and  $P = 1$  atm. The systems consisted of 1000 water molecules and one diamondoid molecule in a cubic box with periodic boundary condition employing the minimum image convention.<sup>10</sup> The simple point charge (SPC)<sup>11</sup> potential was used for the water molecule. The potential model for diamondoid was extensively explored in the light of the small amount of experimental data available.<sup>12,13</sup> Although it has not been possible to systematically parametrize a potential for diamondoids, we found a set of parameters that consistently predicted all structural and energetic properties investigated. The arguments for using the model described below are given in the Results and in the Supporting Information. To obtain a potential model for diamondoids, we first determined the reference geometry from B3LYP/6-311++G(d,p)<sup>14</sup> full optimization for adamantane, diamantane, and trimantane. For the van der Waals parameters, we used sites from OPLS/AA force field.<sup>15</sup> All hydrogen atoms were modeled using van der Waals parameters from the hydrogen alkyl group.<sup>15</sup> The partial charges for electrostatic potential were determined using the CHelpG scheme at MP2/aug-cc-pVDZ level.<sup>16</sup> All parameters of the potential are given in the Supporting Information, including reference geometry, van der Waals parameters, and partial charges.

Properties were calculated from simulations considering a time step of 2 fs with data collected every 0.01 ps. The cubic cells were equilibrated for 500 ps, and for the equilibration process we have performed a running length of 5 ns, both in the NPT ensemble. The system was kept at the appropriate temperature and pressure via velocity rescaling<sup>17</sup> and Parrinello-Rahman<sup>18</sup> schemes, with a constant coupling of 0.1 and 1.0, respectively. All bond lengths were constrained via the LINCS algorithm.<sup>19</sup> A cutoff distance of 1.2 nm for LJ interaction was employed, whereas the Coulomb interactions were treated by using the PME algorithm.<sup>20</sup>

The elucidation of free-energy differences due to changes in intermolecular interactions is an important issue in solution chemistry and could be used here to describe the thermodynamics solvation of diamondoids. Hydration free energy was calculated using the stochastic MD associated with thermodynamic integration scheme<sup>10</sup> by decoupling a solute molecule from the solvent using the identity:

$$\Delta G = \int_{\lambda=0}^{\lambda=1} \frac{dH(\lambda)}{d\lambda} d\lambda$$

where  $H$  is the parametrized Hamiltonian, for which the coupled state ( $\lambda = 1$ ) corresponds to a simulation with the solute fully interacting with the solvent and the uncoupled state ( $\lambda = 0$ ) corresponds to a simulation considering the solute without interaction with the solvent.

For the purpose of avoiding singularities, we have used the soft-core interactions for the LJ interactions:<sup>21–23</sup>

$$V_{SC}(r) = (1 - \lambda)V([\alpha\sigma^6\lambda^p + r^6]^{1/6})$$

where  $V_{SC}(r)$  is the normal hard-core pair potential,  $\sigma$  is the LJ size parameter of the atom pair, and  $\lambda = 0$  and  $\lambda = 1$  correspond to the fully coupled and uncoupled states, respectively. The parameters for the soft-core were  $\alpha = 0.5$ ,  $p = 1.0$ , and  $\sigma = 0.3$ .

For the Langevin thermostat, we have used a friction coefficient of 1 ps<sup>−1</sup>.

The decoupling of both terms, Coulomb and van der Waals, at the thermodynamic integration can lead the system to instabilities during the process.<sup>24</sup> This is because the removal of the van der Waals interactions, while the system maintains some electrostatic charge, allows atoms oppositely charged to interact at close distances, resulting in unstable configurations and unreliable energies even if the system does not collapse. Therefore, a two-steps approach has been recommended:<sup>24</sup> first, decoupling the electrostatic interactions of the solute, retaining only those van der Waals interactions, then decoupling the van der Waals interactions, transforming the solute in a set of completely noninteracting atoms. Thus, we performed for each diamondoid two series of simulations in each solvent: one to decouple the Coulomb interactions and the other to decouple the van der Waals interactions. In each series, 26 values for  $\lambda$  were used, from 0 to 1, uniformly separated by increments of 0.04. For each simulation, the system was equilibrated for 1 ns, followed by a 5 ns run. The solvation free energy was then obtained by summing the energies of each process, that is,  $\Delta G = \Delta G_{Coul} + \Delta G_{vdW}$ .

To obtain quantitative information about the association process of diamondoids in aqueous medium, we calculated the PMF. Here PMF is the function that describes how the free energy between two diamondoids varies as we increase the distance between their centers. To calculate the PMF, we employed the umbrella sampling technique<sup>25</sup> with weighted histogram analysis method (WHAM).<sup>26</sup> This technique requires that a number of restraints be applied at specific positions on the reaction coordinate (in this case the distance between the diamondoid) so that all regions are appropriately sampled. Each specific restrained position consists of a window simulation. In this work, for each diamondoid pair we conducted a series of 23 simulation windows with harmonic restraint of 1000 kJ mol<sup>−1</sup> nm<sup>−2</sup>, where the separation between the centers of mass was increased from 0.35 to 1.45 nm with 0.05 nm increments. Each simulation was 5 ns long, giving a total time of 115 ns for each diamondoid pair. For simulations in vacuum we use exactly the same protocol used for the simulations in water, but in that case we remove the periodic boundary conditions and the cutoffs to the electrostatic and van der Waals interactions.

All stochastic and MD simulations have been performed with the GROMACS 4.5 program.<sup>22,23</sup> Supporting quantum calculations for diamondoids reference structures and for CHelpG charges were performed using the Gaussian 03 program.<sup>27</sup>

## RESULTS

In this work, MD simulation has been performed to investigate the structure, dynamical, and energetic properties of the three first members of the diamondoids series. Before we present our results, it is necessary to discuss in detail the model used here.

**Potential Model.** In the literature, only a small amount of experimental data involving thermodynamic quantities of diamondoids that may serve as basis for a parametrization are available. In particular, there are two experimental values for the partition coefficient of the adamantane. One of these values is the partition coefficient between *n*-hexadecane and vacuum ( $\log P^{\text{hex-vac}} = 4.77$ ), and it corresponds to a solvation-free energy of 27.2 kJ mol<sup>−1</sup>.<sup>13</sup> Another value refers to the 1-octanol/water partition coefficient ( $\log P^{\text{oct-wat}} = 4.24$ ), which

is equivalent to a free energy of transfer between the two solvents of  $24.2 \text{ kJ mol}^{-1}$ .<sup>12</sup> In our preliminary tests (see the Supporting Information), we tried to parametrize a model based on free-energy solvation of the adamantane in *n*-hexadecane. Our adjusted potential parameters reproduced with good accuracy the value for the free energy of solvation of the adamantane in *n*-hexane, finding a value of  $27.1 \text{ kJ mol}^{-1}$ ; however, for the energy transfer between 1-octanol and water, this model provided a value of  $35.3 \text{ kJ mol}^{-1}$ ,  $8.2 \text{ kJ mol}^{-1}$  above the experimental value. In addition, we determined for the hydration free a value of  $-5.3 \text{ kJ mol}^{-1}$ , a negative value that does not reflect the hydrophobic character of adamantane.

This result reflects the difficulty of parametrizing a molecular potential that provides satisfactory values for the transfer free energy between two solvents of different polarities. This difficulty is certainly associated with the limitations of the employed force fields for both adamantane and the organic solvents.<sup>28–30</sup> The use of traditional force fields (parametrized based on the reproduction of the heat of vaporization and density) has provided, for most of the cases, only qualitative concordance with the experimental values of transfer free energy or partition coefficient.<sup>28,30–32</sup> In general, partition coefficients consistently higher compared with experimental values have been found.<sup>30,32</sup> In our case, it is possible that the force fields used do not reproduce correctly the interactions between 1-octanol (or *n*-hexadecane) and adamantane. Additional simulations are needed for a detailed analysis of these interactions and a possible improvement in the force field (where the electrostatic polarization effects can be considered<sup>31</sup>). However, this investigation is outside the scope of this work.

Because the limitations mentioned above prevent a parametrization based strictly on the transfer free energy, the model employed for the diamondoids were chosen based on physical–chemical considerations of these molecules, among the various tested models. Although we do not have experimental value for comparison, we note that this result is not consistent with the hydrophobic nature of adamantane. The most appropriate value for the hydration free energy of small diamondoid should contemplate the fact that the hydrophobic hydration of small molecules is dominated by its entropic term, which implies a positive hydration free energy, characterizing its low water solubility.<sup>33</sup> Moreover, one should take into account the particular topology of the adamantane (and other small diamondoids), which has a smaller solvent accessible surface area (SASA) than other hydrocarbons of similar molecular weight. (For example, SASA for *n*-decane is  $\sim 3.44 \text{ nm}^2$ , whereas adamantane is  $2.49 \text{ nm}^2$ .) Finally, we need take into account the fact that adamantane is a structure formed by three condensed cyclohexane rings fused, making it more reactive than the *n*-alkanes<sup>34,35</sup> and giving it a hydration free energy comparable to that expected for the cyclo-alkanes, which has a SASA slightly higher than adamantane. (For cyclohexane, SASA is  $2.62 \text{ nm}^2$  and  $\Delta G_{\text{hyd}} = 5.14 \text{ kJ mol}^{-1}$ .<sup>36</sup>) All of these aspects were considered in choosing the potential model for the three diamondoids investigated in this work. (See the Supporting Information for further details.)

**Hydration Free Energies.** As mentioned, diamondoids are hydrophobic organic solutes, and thus it is expected that the water solubility of these molecules is extremely low and not measurable with accuracy. Here hydration free energy,  $\Delta G$ , has been calculated to clarify the molecular picture of the hydrophobic hydration of diamondoids. The hydration free

energy and the corresponding enthalpy and entropy contributions are given at Figure 1.

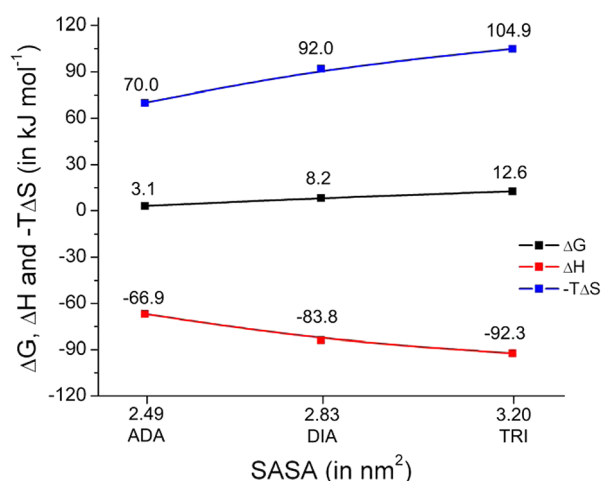


**Figure 1.** Free energy, enthalpy, and entropy (in  $\text{kJ mol}^{-1}$ ) for hydration of the adamantane (ADA), diamantane (DIA), and trimantane (TRI) as a function of the solvent-accessible surface area. The entropic component ( $-T\Delta S$ ) was obtained directly from  $\Delta G = \Delta H - T\Delta S$ . Error estimates in the calculated free energies were obtained by using a block-averaging procedure<sup>37</sup> and are in the range of  $\pm 0.02$  and  $\pm 0.05 \text{ kJ mol}^{-1}$ .

Figure 1 reveals that the thermodynamical behavior of the hydration of the diamondoids is similar to that found for the hydration of *n*-alkanes. For *n*-alkanes, entropic and enthalpic terms are significantly larger regarding the absolute value than the hydration free energies.<sup>33</sup> Moreover, the enthalpies of hydration are large and favorable, whereas the entropies of hydration are large and unfavorable. The entropic terms are systematically higher in absolute value terms than the enthalpy, resulting in unfavorable hydration free energy, which depends linearly on the size of the alkyl chain.<sup>33</sup> For diamondoids, we observed all of these features, including the linear size-dependence, but here the magnitude of the hydration free energy was substantially smaller than that observed for *n*-alkanes. In fact, it could be observed that the migration of a single-molecule diamondoid, from vacuum to water, involved an energy penalty leading to an increase in the hydration free energy of  $3.1 \text{ kJ mol}^{-1}$  for ADA,  $8.2 \text{ kJ mol}^{-1}$  for DIA, and  $12.6 \text{ kJ mol}^{-1}$  for TRI. All of these values are lower than the hydration free energy for *n*-decane, which has molecular weight similar to the adamantane,  $-13.2 \text{ kJ mol}^{-1}$ .<sup>36</sup> It is worth noting here that this difference is not primarily due to the model employed here. Our preliminary simulations showed that the parameters of the force field OPLS/AA, which correctly described the hydration of *n*-alkanes, are not suitable for modeling diamondoids because they provided negative free energy for the adamantane ( $-5.3 \text{ kJ mol}^{-1}$ , see Supporting Information). For diamondoids, the lower relative hydrophobicity can be attributed mainly to its cage-like structure, which provides a considerably smaller SASA (as discussed above) and hence smaller hydration free energy.

Relative hydration free energies tend to reduce the systematic errors because of the force-field limitations. Figure 2 displays these differences for free energy and its enthalpic and entropic contributions. As can be seen, the migration of a single ADA molecule, from vacuum to water, involved an energy cost of  $5.1$





**Figure 2.** Relative hydration free energies (in kJ mol<sup>-1</sup>) for the hydration process of the investigated diamondoids.

kJ mol<sup>-1</sup> lower than the energy required for the migration of DIA molecule. This difference was 4.4 kJ mol<sup>-1</sup> when we considered the migration into water of the DIA and TRI molecules. Furthermore, our calculations also provide an enthalpy difference of -16.9 kJ mol<sup>-1</sup> (between the hydration of ADA and DIA) and -8.5 kJ mol<sup>-1</sup> (between the hydration of the DIA and TRI). An analysis of the entropic component showed a similar trend (although with opposite sign). From these findings, we observed that as the size of diamondoid increases, the enthalpic gain decreases proportionally to the decrease in entropic loss. This linear behavior is expected for such differences from the small hydrophobic solute. Although, above a critical size, it should occur as an inversion, and hydrophobicity should be dominated by enthalpic rather than entropic factors.

**Potential of Mean Force.** Aiming at the investigation of the association of pairs of diamondoids in aqueous solution, we determined the PMF for the center of mass distance. Figure 3 presents the PMFs in vacuum and water for the three diamondoids. In vacuum, as expected, it was observed that the interaction between the diamondoids depended on its size, following the order: ADA (-8.2 kJ mol<sup>-1</sup>), DIA (-9.9 kJ mol<sup>-1</sup>), and TRI (-12.6 kJ mol<sup>-1</sup>). The contact minima were placed at positions that progressively increased according to the size of diamondoid: 0.68 (ADA), 0.70 (DIA), and 0.72 nm (TRI).

It is interesting to note that despite the PMF in vacuum preserving all of the essential features of a LJ-type potential, it presented a broader potential well for the DIA and TRI. This is evidence of how the PMF depends on the solute shape. The DIA molecule, for example, is a more elongated particle compared with ADA, so that its PMF was sampled over all possible relative orientations between the two molecules of the dimer, which caused the enlargement of the potential well. A comparison of the PMFs in vacuum and in water showed that in all cases the water destabilizes the interaction of the dimers, reducing significantly the depth of the well. This result is consistent with the finding of Scheraga et al.,<sup>38</sup> who showed

that for hydrophobic solutes with carbon numbers greater than 5 the PMF in water is shallower than the PMF in vacuum. Furthermore, we noted that the PMF in water has minimum contact with the three diamondoids, indicating that these molecules tend to aggregate spontaneously in water, which is consistent with its hydrophobicity. The deep contact minima in the PMF were calculated as -6.8, -5.8, and -7.5 kJ mol<sup>-1</sup> for ADA, DIA, and TRI, respectively, placed at the distances 0.66, 0.72, and 0.72 nm between the centers of mass of the two diamondoids. The minimum found here for ADA is comparable to the value found by Scheraga et al., which was -7.3 kJ mol<sup>-1</sup>.<sup>38</sup> Additionally, we also observed a desolvation barrier of 1.6, 1.7, and 1.5 kJ mol<sup>-1</sup>, separating a shallow solvent separated minimum for each PMF at the distances 0.86, 0.92, and 1.00 nm for ADA, DIA, and TRI, respectively. As can be seen, these distances are progressively displaced from each other and depend on the size of diamondoid. The contribution of the solvent for the stabilization of the dimers was important here. Initially, we observed that the depth of the potential well did not depend only on the solute size. The contact minimum for DIA, for example, is shallower than that for ADA, which has a lower molecular weight, whereas the minimum for TRI is only slightly deeper than that for ADA. Unlike what happens for small hydrophobic solutes, where the contribution of the solvent has a clear maximum in the desolvation position, here this contribution occurred in the rough plateaus in the region of the potential well for the two largest analyzed diamondoids (Figure 4).

These observations suggest that the format of diamondoids and its possible relative orientations in the dimer can alter the local structure of hydration, leading to the variations on the stability of the dimer.

## CONCLUSIONS

MD simulations were used to investigate the thermodynamics behavior of the hydration of the three smallest diamondoids. We observed features in common with *n*-alkanes, including the linear size dependence, but the magnitude of the hydration free energy was substantially smaller. Because diamondoids are structures formed by condensed cyclohexane rings fused, they are more reactive than the *n*-alkanes and present hydration free energy comparable to that expected for the cyclo-alkanes of similar SASA.

PMF calculations were performed to investigate the association and aggregation of pairs of diamondoids in aqueous

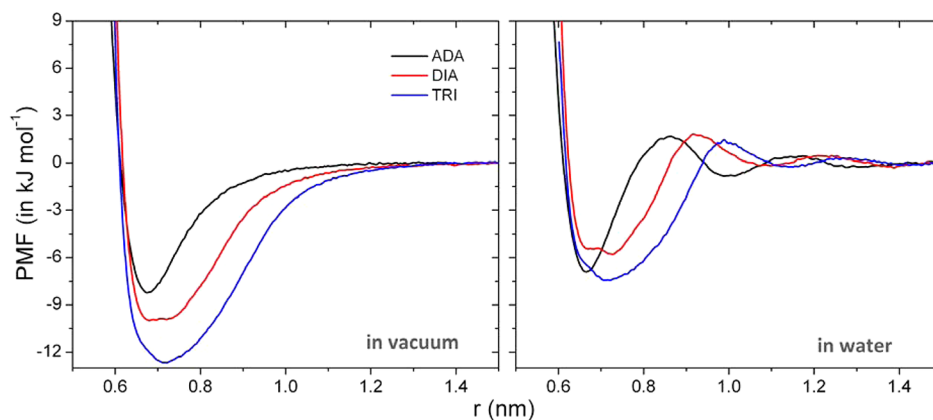


**Figure 3.** Potential of mean force (in kJ mol<sup>-1</sup>) for the diamondoid dimers in vacuum and in water. PMFs are set to zero at a separation of 1.5 nm.

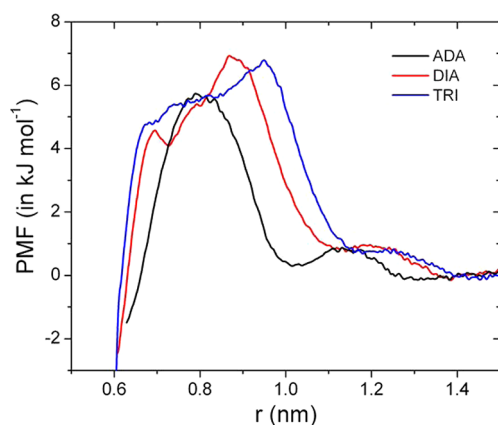


**Figure 4.** Water-induced contribution to the PMF (in  $\text{kJ mol}^{-1}$ ) obtained by subtracting the PMF in vacuum from the PMF in water.

solution. We found that the PMF in water has minimum contact for the three diamondoids, indicating that these molecules tend to aggregate spontaneously in water, which is consistent with its hydrophobicity. Also, we observed that the water-induced contribution is repulsive for all diamondoid and in practically every interval of separation of the centers of mass. This contribution represents a significant portion of the PMF, especially for DIA and TRI, and is responsible for the reduction of the interaction of dimers in aqueous media.

To our knowledge, there are no experimental data at room conditions that characterize the thermodynamics of the hydration of diamondoids. Moreover, this is the first systematic computational work on these systems in condensed phase. Therefore, we believe that the results presented here will be useful for both future experimental predictions and the development of new computational investigations on these species.

## ■ ASSOCIATED CONTENT

### ● Supporting Information

Extensive tests on quality of potential models for diamondoids are shown in detail. All parameters for the models employed are supplied along with the reference geometries for each diamondoid. Further analysis on the structure of the solutions and the calculations convergence is also provided. This material is available free of charge via the Internet at <http://pubs.acs.org>.

## ■ AUTHOR INFORMATION

### Corresponding Author

\*E-mail: [fileti@unifesp.br](mailto:fileti@unifesp.br). Tel: +55 12 3309-9573. Fax: +55 12 3921-8857.

### Notes

The authors declare no competing financial interest.

## ■ ACKNOWLEDGMENTS

This work was supported by grants from Brazilian agencies FAPESP and CNPq. We thank Dr. Dayane Tada for her critical review and comments.

## ■ REFERENCES

- (1) Dahl, J. E.; Liu, S. G.; Carlson, R. M. K. *Science* **2003**, *299*, 96–99.
- (2) Marchand, A. P. *Science* **2003**, *299*, 52–53.
- (3) Schwertfeger, H.; Fokin, A. A.; Schreiner, P. R. *Angew. Chem., Int. Ed.* **2007**, *47*, 1022–1036.

- (4) Dahl, J. E.; Moldovan, J. M.; Peters, K. E.; Claypool, G. E.; Rooney, M. A.; Michael, G. E.; Mello, M. R.; Kohnenk, M. L. *Nature* **1999**, *399*, 54–57.
- (5) Drummond, N. D.; Williamson, A. J.; Needs, R. J.; Galli, G. *Phys. Rev. Lett.* **2005**, *95*, 096801.
- (6) Byrappa, K.; Adschi, T. *Prog. Cryst. Growth Charact. Mater.* **2007**, *53*, 117–166.
- (7) Chan, Y. C.; Choy, K. K. H.; Chan, A. H. C.; Ng, K. M.; Liu, S.; Sciamanna, S. F.; Dahl, J. E.; Carlson, R. M. K. *J. Chem. Eng. Data* **2008**, *53*, 1767–1771.
- (8) Cansell, F.; Aymonier, C. *J. Supercrit. Fluids* **2009**, *47*, 508–516.
- (9) Sobolewski, E.; Makowski, M.; Czaplewski, C.; Liwo, A.; Oldziej, S.; Scheraga, H. A. *J. Phys. Chem. B* **2007**, *111*, 10765–10774.
- (10) Leach, A. *Molecular Modelling: Principles and Applications*; Prentice Hall: New York, 2001.
- (11) Berendsen, H. J. C.; Postma, J. P. M.; van Gunsteren, W. F.; Hermans, J. In *Intermolecular Forces*; Pullman, B., Ed.; Reidel: Dordrecht, The Netherlands, 1981.
- (12) Marti, J.; Gordillo, M. C. *Chem. Phys. Lett.* **2002**, *354*, 227–232.
- (13) Skarmoutsos, I.; Guardia, E. *J. Chem. Phys.* **2010**, *132*, 074502–074512.
- (14) Koch, W.; Holthausen, M. C. *A Chemist's Guide to Density Functional theory*; Wiley-VHC: New York, 2001.
- (15) Jorgensen, W. L.; Maxwell, D. S.; Tirado-Rives, J. *J. Am. Chem. Soc.* **1996**, *118*, 11225–11236.
- (16) Breneman, C. M.; Wiberg, K. B. *J. Comput. Chem.* **1990**, *11*, 361–373.
- (17) Bussi, G.; Donadio, D.; Parrinello, M. *J. Chem. Phys.* **2007**, *126*, 014101–014108.
- (18) Parrinello, M.; Rahman, A. *J. Appl. Phys.* **1981**, *52*, 7182–7191.
- (19) Hess, B.; Bekker, H.; Berendsen, H. J. C.; Fraaije, J. G. E. M. *J. Comput. Chem.* **1997**, *18*, 1463–1472.
- (20) Darden, T.; York, D.; Pedersen, L. *J. Chem. Phys.* **1993**, *98*, 10089–10093.
- (21) Beutler, T. C.; Mark, A. E.; van Schaik, R. C.; Greber, P. R.; van Gunsteren, W. F. *Chem. Phys. Lett.* **1994**, *222*, 529–539.
- (22) Lindahl, E.; Hess, B.; van der Spoel, D. *J. Mol. Model.* **2001**, *7*, 306–317.
- (23) Berendsen, H. J. C.; van der Spoel, D.; van Drunen, R. *Comput. Phys. Commun.* **1995**, *91*, 43–56.
- (24) Shirts, M. R.; Pitera, J. W.; Swope, W. C.; Pande, V. S. *J. Chem. Phys.* **2003**, *119*, 5740–5761.
- (25) Torrie, G. M.; Valleau, J. P. *J. Comput. Phys.* **1977**, *23*, 187–199.
- (26) Kumar, S.; Bouzida, D.; Swendsen, R. H.; Kollman, P. A.; Rosenberg, J. M. *J. Comput. Chem.* **1992**, *13*, 1011–1021.
- (27) Frish, M. J.; Trucks, G. W.; Schlegel, H. B.; Scuseria, G. E.; Robb, M. A.; Cheeseman, J. R.; Montgomery, J. A., Jr.; Vreven, T.; Kudin, K. N.; Burant, J. C.; et al. *Gaussian 03*; Gaussian, Inc.: Wallingford CT, 2003.
- (28) Matubayasi, N.; Wakai, C.; Nakahara, M. *J. Chem. Phys.* **1997**, *107*, 9133–9140.
- (29) Liu, Y.; Li, X.; Wang, L.; Sun, S. *Fluid Phase Equilib.* **2009**, *285*, 19–23.
- (30) Chialvo, A. A.; Cummings, P. T. *J. Chem. Phys.* **1994**, *101*, 4466–4469.
- (31) Matubayasi, N.; Wakai, C.; Nakahara, M. *J. Chem. Phys.* **1999**, *110*, 8000–8012.
- (32) Gao, J. *J. Am. Chem. Soc.* **1993**, *115*, 6893–6895.
- (33) Townsend, S. H.; Abraham, M. A.; Gilbert, I.; Huppert, L.; Klein, M. T.; Paspekt, S. C. *Ind. Eng. Chem. Res.* **1988**, *27*, 143–149.
- (34) Plugatyr, A.; Nahtigal, I.; Svishchev, I. M. *J. Chem. Phys.* **2006**, *124*, 024507–024516.
- (35) Su, Z.; Maroncelli, M. *J. Chem. Phys.* **2006**, *124*, 164506–164521.
- (36) Kiselev, M.; Ivlev, D. *J. Mol. Liq.* **2004**, *110*, 193–199.
- (37) Hess, B. *J. Chem. Phys.* **2002**, *116*, 209–218.
- (38) Makowski, M.; Czaplewski, C.; Liwo, A.; Scheraga, H. A. *J. Phys. Chem. B* **2010**, *114*, 993–1003.